A Single-Stage Solar PV Power Fed Open-End Winding Induction Motor Pump Drive with MPPT

Ramsha Karampuri, Sachin Jain, V. T. Somasekhar, *Member IEEE*
Department of Electrical Engineering,
National Institute of Technology,
Warangal – 506004, INDIA
ramsha_k@nitw.ac.in, jsachin@nitw.ac.in, vtsomasekhar@rediffmail.com

***Abstract*—In this paper a single-stage solar PhotoVoltaic (PV) system feeding the power to an Open-End Winding Induction Motor (OEWIM) *via* a dual-inverter is presented. The OEWIM is coupled to a centrifugal pump for water pumping application. The dual-inverter fed OEWIM is chosen, as it requires low dc-bus voltage which helps in optimal arrangement of PV modules, which could avoid large strings. In the proposed system a single PV source is connected to both the inverters, which results in zero-sequence current and hence the harmonics in the system. So as to nullify the zero-sequence current in the average sense Sample-Averaged Zero-sequence Elimination (SAZE) Pulse Width Modulation (PWM) technique is adopted. This algorithm ensures the clamping of one of the inverter when the other is being switched; this reduces the switching losses and efficiency may increase which is important factor to be considered in PV system. Also the above algorithm reduces the current ripple at higher modulation indices. The modulation index is tuned by using Maximum Power Point Tracking (MPPT) algorithm for the variations in the insolation and ambient temperature. The detailed explanation of the control algorithm for the proposed system and its simulation results under different environmental conditions are presented.**

Keywords—maximum power point tracking; nearest sub-hexagonal centre; open-end winding induction motor; photovoltaic; pulse width modulation; sample-averaged zero-sequence elimination.

I. INTRODUCTION

The application of renewable energy sources, especially solar PhotoVoltaic (PV) is becoming increasingly popular in rural areas where power from the utility is not available. This has adverse effect on agriculture due to lack of water in the summer. The solar PV power fed water pumps could provide a possible solution to meet the water requirement in the fields during summer. G. Vetter *et. al*. [1] had proven the suitability of the photovoltaic power to drive water pumps. Later Eduard Muljadi [2] had proposed a water pumping system with PV array supplying power to a three-phase square wave inverter fed induction motor drive which is connected to a centrifugal water pump. However, the line current in the system proposed by Eduard Muljadi [2] contain predominant third order harmonics.

To reduce the harmonics and to increase the efficiency of the induction motor drive system Akira Nabae *et. al.* [3] had proposed a three-level neutral-point clamped inverter. As the level of output voltage increases, the complexity in the power circuit as well as the cost increases. H. Stemmler *et. al*. [4] had proposed a three-level Voltage Source Inverter (VSI) by connecting two 2-level VSIs (dual-inverter) to the either ends of an Open-End Winding Induction Motor (OEWIM) to reduce the complexity of the induction motor drive system. The authors used sine triangle Pulse Width Modulation (PWM) technique in their proposed system. Later E. G. Shivakumar *et. al.* [5] had suggested Space Vector PWM (SVPWM) technique for the dual-inverter fed OEWIM. In the given proposal the authors have used two separate DC power supplies to eliminate the zero-sequence current. Based on this strategy different PWM techniques were introduced by V. T. Somasekhar *et. al*. [6], Baiju *et. al.* [7], Oleschuk *et. al.* [8]. Since the suggested techniques did not use all the space vector locations resulting in underutilisation of the switching resources, V. T. Somasekhar *et. al.* [9] proposed a PWM switching strategy with a single DC source fed dual-inverter driven OEWIM as shown in Fig. 1. In their manuscript Sample-Averaged Zero-sequence Elimination (SAZE) PWM technique was proposed to balance the zero-sequence current dynamically by making zero-sequence voltage to zero, in average sense, within a sampling time interval.

This manuscript extends the concept of SAZE PWM technique and integrates it with MPPT algorithm to the system with a PV source feeding power to OEWIM which is coupled to a centrifugal pump as shown in Fig. 2. A single PV source is used in the proposed system which supplies power to two two-level inverters which are connected to the either ends of OEWIM (Fig. 2). As there is a common DC-link to both the inverters, it results in zero-sequence current, and hence the harmonics, which are undesirable with respect to both the PV

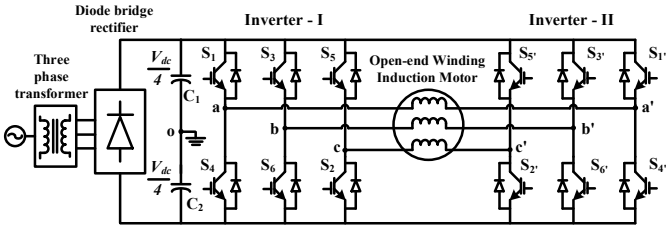

Fig. 1. OEWIM connected to dual two-level inverter with a single DC power supply.

978-1-4799-6373-7/14/$31.00 ©2014 IEEE

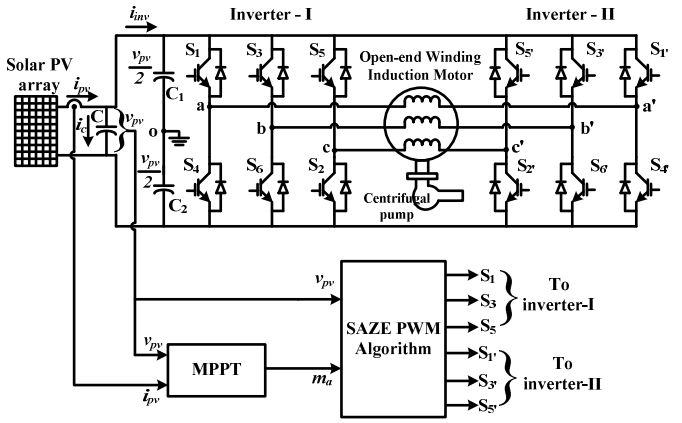

Fig. 2. Single-stage single solar PV source supplying power to dual-inverter fed OEWIM driven water pump system.

source and the motor. For the purpose SAZE PWM technique is adopted for the proposed system.

In the following sections, a brief explanation of the proposed control algorithm which integrates MPPT and SAZE PWM technique is presented. Also, the proposed system is simulated using MATLAB/Simulink under different environmental conditions and the behaviour of the system is explained in the results section. Conclusions are presented in the last section.

II. System Description and Control Algorithm

The proposed system shown in Fig. 2, consists of a solar PV array, a dual-inverter (namely inverter-I and inverter-II), three-phase induction motor with open-end windings, centrifugal pump connected to the OEWIM rotor shaft, MPPT block and SAZE PWM algorithm block. All the blocks mentioned above are discussed briefly in the following sub-sections.

A. Solar PV array

A single PV source is used to supply the power to the pump drive. The solar PV array supplies current, i_{pv} given by equation (1) as

$$i_{pv} = N_p i_{sc} - N_p i_s \left[e^{\frac{q(v_{pv}+i_{pv}R_s)}{N_s AkT}} - 1 \right] - \frac{\left[\frac{v_{pv}}{N_s} + i_{pv} R_s \right]}{R_p} \qquad (1)$$

where i_{sc} is the PV cell short circuit current (A), i_s is the diode reverse saturation current (A), N_p is the number of parallel connected PV cells, N_s is the number of series connected PV cells, A is the diode ideality factor, k is the boltzmann constant (J/K), q is the electron charge (C), T is the panel operating temperature (K), R_s is the series resistance of the cell and R_p is the parallel resistance of the cell, v_{pv} is the PV voltage.

B. OEWIM and centrifugal pump

The stator phase windings of a simple three-phase induction motor are opened from both the ends and connected to the inverter output terminals as shown in Fig. 2. The OEWIM is mechanically coupled to a centrifugal pump used for pumping water. The combined torque dynamics of OEWIM and pump can be described by the equation (2) as

$$T_{em} = J \frac{d\omega_r}{dt} + B\omega_r^{\,2} \qquad (2)$$

where T_{em} is the electromechanical torque developed by the motor (N-m), ω_r is the speed of the rotor (rps), J is the moment of inertia (kg-m^2) and B is the coefficient of friction.

The centrifugal pump is governed by the following *Affinity Laws*

$$\begin{aligned} Q &\propto \omega_r \\ H &\propto \omega_r^2 \\ P &\propto \omega_r^3 \end{aligned} \qquad (3)$$

where Q is the flow rate in m^3/s, H is the head in m and P is the power in W.

C. Control algorithm

In the proposed single-stage PV pumping system, a simple control algorithm is used to track the maximum power from the PV source as well as to drive the dual-inverter fed OEWIM pump. For the purpose, MPPT algorithm is integrated with the SAZE PWM technique which is presented in the form of a flow chart as shown in Fig. 3. Both the sub-blocks of Fig. 3 i.e., MPPT and SAZE PWM are explained below.

1) Maximum power point tracking

The most popular method of tracking maximum power is the hill climbing algorithm proposed by B. K. Bose *et. al.* [10]. As the hill climbing algorithm is simple, robust and accurate it is mostly used for MPPT [11]. The instantaneous values of PV current, i_{pv} and PV voltage, v_{pv} are multiplied to get the instantaneous PV power, p_{pv} supplied to the dual-inverter. Using which the operating point at maximum power for all the environmental conditions is determined and the required modulation index, m_a for the PWM algorithm is calculated as shown in Fig. 3.

2) Sample-Averaged Zero-sequence Elimination PWM

Inverter-I and inverter-II of Fig. 2 are the two-level inverters, which are combined to generate a three-level motor phase voltages v_{aa}□, v_{bb}□, v_{cc}□ [9]. Each inverter individually can produce the phase voltage with a peak value of v_{pv} (OA) and together can produce $2v_{pv}$ (OG) as shown in Fig. 4. The magnitude of the reference voltage vector OT (Fig. 4) is dependent on the value of modulation index (equation (4)) which is generated by MPPT block depending on the insolation and ambient temperature.

$$|v_{sr}| = m_a v_{pv} \qquad (4)$$

The value of $|v_{sr}|$ calculated using equation (4) and the value of m_a generated by MPPT block are used by the SAZE PWM algorithm which is explained briefly in the flowchart shown in Fig. 3.

The inverter switches are operated by the gate pulses generated from the SAZE PWM algorithm block shown in Fig. 2. Basic algorithm used is the one proposed by Joohn-

Sheok Kim et. al. [12,13] for space vector PWM where in effective time concept is introduced, it is extended to dual-inverter. In Fig. 4, A, B, C, D, ... S represents the space vector locations and each equilateral sub-triangle is a sector. The space vector locations A, C and E are considered as Nearest Sub-Hexagonal Centres (NSHC) for inverter-I to be

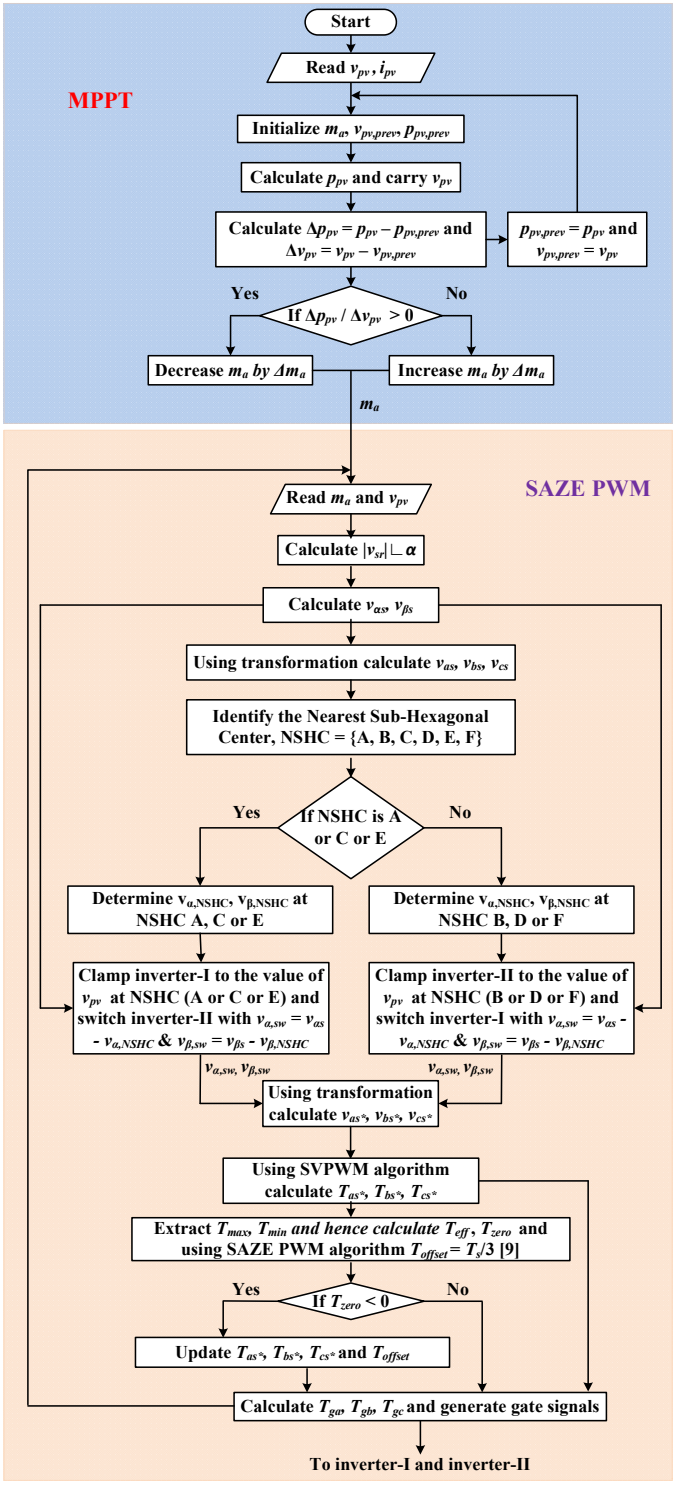

Fig. 3. Flow chart of the integrated MPPT and SAZE PWM algorithm.

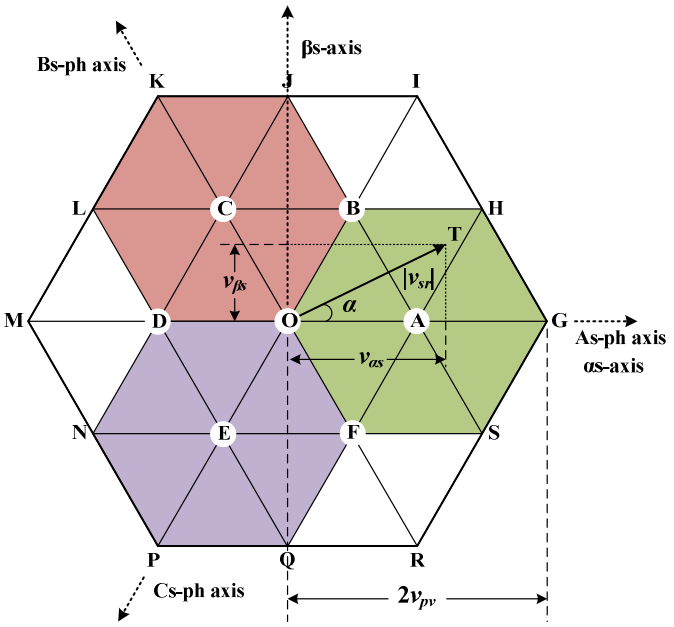

Fig. 4. Space vector locations with the combination of inverter-I and inverter-II.

clamped to the magnitude of $v_{\alpha,NSHC}$ and $v_{\beta,NSHC}$ and inverter-II being switched. Similarly the locations B, D and F are considered as NSHCs for inverter-II to be clamped to the magnitude of $v_{\alpha,NSHC}$ and $v_{\beta,NSHC}$ and inverter-I being switched as shown in Fig. 3. The values of $v_{\alpha,NSHC}$ and $v_{\beta,NSHC}$ at all the NSHCs for inverter-I and inverter-II when they are clamped are shown in Table I.

As shown in the Fig. 3 the offset time period used for the SAZE PWM is

$$T_{offset} = \frac{T_s}{3} \tag{5}$$

where T_s is the sampling time period.

TABLE I. VOLTAGE VECTOR MAGNITUDES AT ALL THE NSHCS

NSHC / Vector	A	B	C	D	E	F
$v_{\alpha,NSHC}$	v_{pv}	0.5 v_{pv}	-0.5 v_{pv}	- v_{pv}	-0.5 v_{pv}	0.5 v_{pv}
$v_{\beta,NSHC}$	0	0.867 v_{pv}	0.867 v_{pv}	0	-0.867 v_{pv}	-0.867 v_{pv}

III. SIMULATION RESULTS AND DISCUSSION

The simulation of proposed system is done in MATLAB/Simulink using the parameters shown in Table II. In the simulation, SAZE PWM algorithm is programmed by considering 48 samples per cycle, this result in 2.4 kHz switching frequency for the inverters. The switching and clamping behaviour of inverter-I and inverter-II are presented in Fig. 5(a). The clamping behaviour of both the inverters reduces the switching losses. The top plot of Fig. 5(a) shows the gate pulses for inverter-I and the bottom plot shows the gate pulses for inverter-II. The top plot of Fig. 5(b)

TABLE II. MOTOR AND SOLAR PV ARRAY PARAMETERS

Parameter	Value	Unit
Motor parameters		
Rated voltage (RMS)	400	V
Frequency	50	Hz
Rated speed	1430	rpm
Stator winding resistance, r_s	6.564	Ω
Rotor winding resistance, r_r	4.683	Ω
Leakage reactance, $x_{ls} = x_{lr}$	9.733	Ω
Magnetizing reactance, x_m	196.64	Ω
Poles, p	4	
Solar PV array parameters		
V_{oc} of a PV module	21.1	V
I_{sc} of a PV module	3.8	A
No. of modules in the array	20X3	

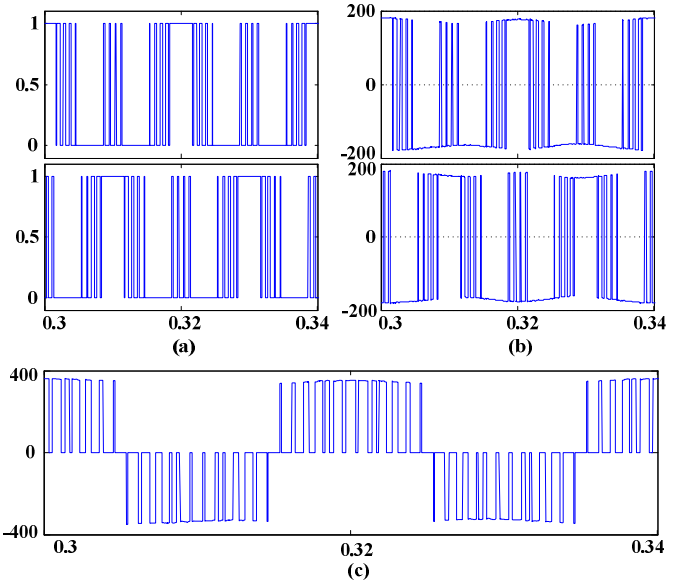

Fig. 5. (a) Gate pulses of inverter-I (top) and gate pulses of inverter-II (bottom), (b) pole voltage, v_{ao} of inverter-I (top) and pole voltage, $v_{a'o}$ of inverter-II (bottom), (c) motor aa'-phase voltage, $v_{aa'}$.

is the pole voltage, v_{ao} (Fig. 2) of inverter-I and the bottom plot is the pole voltage, $v_{a'o}$ (Fig. 2) of inverter-II. Fig. 5(c) is the phase voltage, $v_{aa'}$ of the motor.

The proposed system is simulated for different insolation levels and ambient temperatures to show the performance under all dynamic conditions. Initially, the insolation considered is 0.7 Suns and temperature 30ºC for 1s, and then insolation is increased to 1 Sun and temperature to 35ºC for next 1s. Later from 2 to 3 seconds the insolation is kept constant at 0.5 Suns and temperature at 25ºC. The parameters of a 4.5kW three phase induction motor is chosen for simulation (Table II). The centrifugal pump as a load (equations (3) and (4)) to the motor is connected throughout the simulation i.e., motor is operated with continuous pump load.

The solar PV side waveforms are presented in the Fig. 6, which consists of six sub-plots (insolation, temperature, PV array voltage (v_{pv}), PV array current (i_{pv}), PV array power (p_{pv}) and the modulation index (m_a)). The change in insolation and ambient temperature will change the v_{pv} and i_{pv} thereby p_{pv} which can be observed from the Fig. 6. Maximum power is extracted from the PV array by tuning m_a, which is shown in the last sub-plot of Fig. 6. The nature of m_a (shown as zoom-in part in the last sub-plot of Fig. 6) depicts the tracking of maximum power from PV source and the operating point is oscillating at MPP. The tracked power is then fed to the motor-pump load system.

In Fig. 7, motor side waveforms are plotted i.e., motor phase voltage, phase current, the electromechanical torque developed by the motor and the speed of the motor-pump drive. All the waveforms shown in Fig. 7 are presented with all the dynamic conditions as above. From time 0s to 1s when insolation is 0.7 Suns, the torque ripple and oscillations in the motor speed are medium. When insolation is increased to 1 Sun after 1s, till 2s there is less ripple content in the torque and negligible speed oscillations i.e., motor is running smoothly with a constant speed. Again when insolation is reduced to 0.5 Suns at 2s, the increment in the torque ripple and speed oscillations can be observed from the third and fourth subplots of Fig. 7. So, it is observed that the torque ripple and oscillations in the motor speed decreases with increase in the insolation. The ripple content in the torque is because of the ripple in the current flowing through the motor windings.

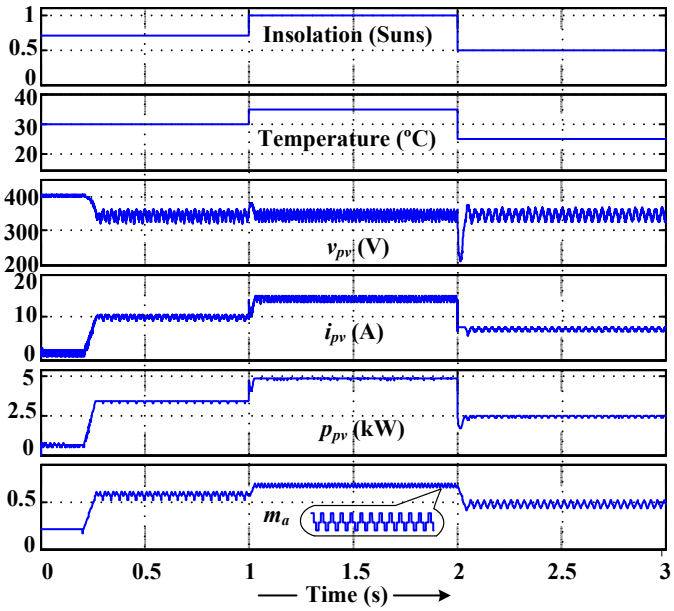

Fig. 6. Solar PV source side waveforms.

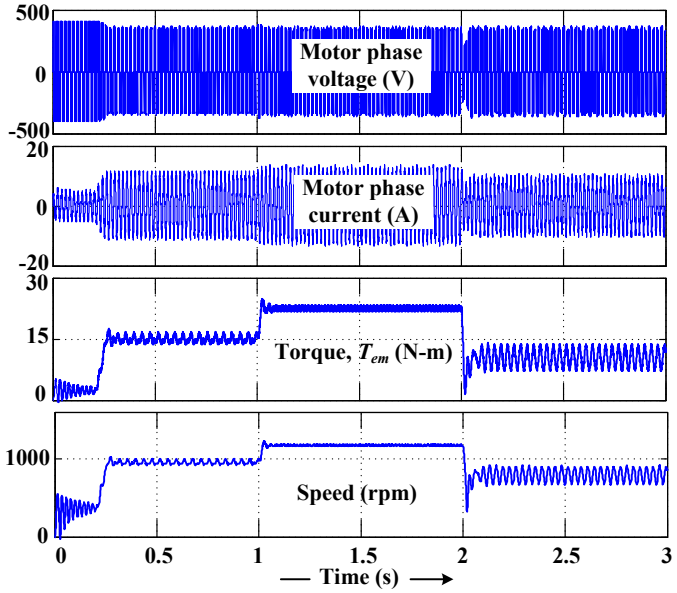

Fig. 7. OEWIM-pump side waveforms.

The motor phase current shown in Fig. 7 is zoomed in and presented in Fig. 8 (a-d) along with its harmonic spectrum under different insolation and temperature conditions. It can be further verified from the waveforms shown in Fig. 8, the ripple content in the current decrease with increase in the insolation. Fig. 8(a) shows the motor phase current waveform at starting condition (0.1s). It can be observed that even in transient state (starting of motor) the THD of motor current is appreciable. Also the ripple content in the motor phase current is very less in Fig. 8(c) at insolation of 1 Sun. The conclusions from Fig. 8(a-d) are presented in Table III.

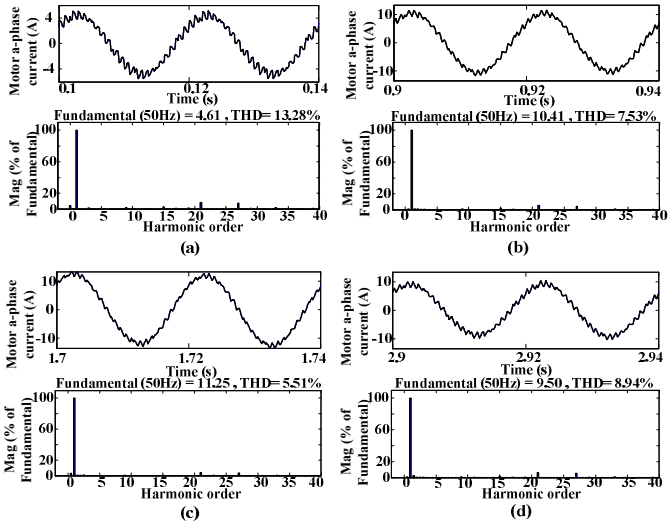

Fig. 8. (a-d) Motor *aa'*-phase current (top) and its harmonic spectrum (bottom) for different time intervals.

TABLE III. OBSERVATIONS FROM FIG. 8 (A-D)

Fig.	Time (s)		Insolation (Suns)	Temperature (°C)	Current ripple	THD (%)
	From	*To*				
8(a)	0.1	0.14	0.7	30	High[a]	13.28
8(b)	0.9	0.94	0.7	30	Medium	7.53
8(c)	1.7	1.74	1.0	35	Very less	5.51
8(d)	2.9	2.94	0.5	25	High	8.94

[a] Under transient condition.

IV. CONCLUSION

A single PV source fed dual-inverter connected to an open-end winding induction motor driving a water-pump load is proposed in this paper. In this single-stage system the inherent twice voltage boosting capability helps in optimally arranging the PV modules, avoiding large strings. The zero-sequence current which is generated due to the common DC-link for dual-inverter is undesirable for the PV source and also to the motor. To dynamically balance the zero-sequence current and also to reduce the switching losses in the inverter, the SAZE PWM technique is adopted and integrated to the MPPT algorithm. The behavior of the proposed system under various dynamic environmental conditions has been presented. The maximum power is extracted from the PV source under various conditions mentioned above using hill climbing algorithm. The ripple content in the torque and the oscillations in the motor speed at different insolation and temperature are presented. From this paper it can be concluded that the harmonics in the motor phase current can be reduced by using SAZE PWM technique for a PV system, also the ripple content in the current and the total harmonic distortion (THD) is very less at higher insolation.

REFERENCES

[1] G. Vetter and W. Wirth, "Suitability of Eccentric helical pumps for turbid water deep well pumping in photovoltaic systems," *Solar Energy*, vol. 51, pp. 205-214, 1993.

[2] Eduard Muljadi, "PV water pumping with a peak-power tracker using a simple six-step square-wave inverter," *IEEE Trans. Ind. Appl.*, vol. 33, no. 3, pp. 714-721, May/June 1997.

[3] Akira Nabae, Isao Takahashi and Hirofumi Akagi, "A new neutral-point-clamped PWM inverter," *IEEE Trans. Ind. Appl.*, vol. IA-17, no. 5, pp. 518-523, Sept./Oct. 1981.

[4] H. Stemmler and P. Guggenbach, "Configurations of high-power voltage source inverter drives", *Proc. of EPE conf.*, pp. 7-12, 1993.

[5] E. G. Shivakumar, K. Gopakumar, S. K. Sinha, Andrei Pittet and V. T. Ranganathan, "Space vector PWM control of dual inverter fed open-end winding induction motor drive," *EPE Journal*, vol. 12, no. 1, pp. 9-18, 2002.

[6] V. T. Somasekhar, K. Gopakumar, E. G. Shivakumar and S. K. Sinha, "A space vector modulation scheme for a dual two level inverter fed an open-end winding induction motor drive for the elimination of zero-sequence currents," *EPE Journal*, vol. 12, no. 2, pp. 26-36, 2002.

[7] M. R. Baiju, K. K. Mohapatra, R. S. Kanchan and K. Gopakumar, "A dual two level inverter scheme with common mode voltage elimination for an induction motor drive," *IEEE Trans. Power Elect.*, vol. 19, no. 3, pp. 794-805, May 2004.

[8] V. Oleschuk, B. K. Bose and A. M. Stankovic, "Phase-shift-based synchronous modulation of dual inverters for an open-end winding induction motor drive with elimination of zero-sequence currents," *Conf. Proc. IEEE-PEDS*, pp. 325-330, Nov./Dec. 2005.

[9] V. T. Somasekhar, S. Srinivas, B. Prakash Reddy, Ch. Nagarjuna Reddy and K. Sivakumar, "Pulse width-modulated switching strategy for the dynamic balancing of zero-sequence current for a dual inverter fed open-end winding induction motor drive," *IET Elec.l Power Appl.*, vol. 1, no. 4, pp. 591-600, July 2007.

[10] B. K. Bose, P. M. Szczesny and R. L. Steigerwald, "Microcomputer control of a residential photovoltaic power conditioning system," *IEEE Trans. Ind. Appl.,* vol. IA-21, no. 5, pp. 1182–1191, Sept./Oct.1985.

[11] S. Jain and V. Agarwal, "Comparison of the performance of maximum power point tracking schemes applied to single-stage grid-connected photovoltaic systems," *IET Elect. Power Appl.*, vol. 1, no. 5, pp. 753-762, Sept. 2007.

[12] J.-S. Kim and S.-K. Sul, "A novel voltage modulation technique of the space vector PWM," *Conf. Proc. IPEC*, pp. 742-747, 1995.

[13] D.-W. Chung, J.-S. Kim and S.-K. Sul, "Unified voltage modulation technique for real-time three-phase power conversion," *IEEE Trans. Ind. Appl.*, vol. 34, no. 2, pp. 374–380, March/April 1998.

[14] S. Srinivas and V. T. Somasekhar, "A new alternate-inverter PWM switching strategy for reducing the common-mode voltages for a dual-inverter fed open-end winding induction motor drive," *Conf. Proc. IPEC, Niigata, Japan*, pp. 1460-1465, 2005.